Mex3a Marks a Slowly Dividing Subpopulation of Lgr5+ Intestinal Stem Cells

HHS Public Access

Author manuscript

Cell Stem Cell. Author manuscript; available in PMC 2018 January 19.

Published in final edited form as:

Cell Stem Cell. 2017 June 01; 20(6): 801–816.e7. doi:10.1016/j.stem.2017.02.007.

Mex3a marks slow-proliferating multilineage progenitors of the intestinal epithelium

Francisco M. Barriga[1], **Elisa Montagni**[1], **Miyeko Mana**, **Amy Guillaumet-Adkins**, **Xavier Hernando-Momblona**[1], **Marta Sevillano**[1], **Gustavo Rodriguez-Esteban**, **Maria Mendez-Lago**, **Simon J. A. Buczacki**[2], **Ivo Gut**, **Marta Gut**, **Douglas J. Winton**[2], **Omer Yilmaz**, **Camille Stephan-Otto**[1], **Holger Hein**, and **Eduard Batlle**[1,3]

[1]Institute for Research in Biomedicine (IRB Barcelona), The Barcelona Institute of Science and Technology. Baldiri Reixac 10, 08028 Barcelona, Spain

[2]Cancer Research UK Cambridge Research Institute, Li Ka Shing Centre, Robinson Way, Cambridge CB2 0RE, UK

[3]Institució Catalana de Recerca i Estudis Avançats (ICREA), Pg. Lluís Companys 23, 08010 Barcelona, Spain

[4]Omer/Miyeko

[5]CNAG

SUMMARY

The intestinal epithelium is continuously regenerated by highly proliferative Lgr5+ intestinal stem cells (ISCs). The existence of a population of quiescent ISCs has been suggested yet its identity and features remain controversial. Here we describe that the expression of the RNA-binding protein Mex3a labels a subpopulation of Lgr5+ cells that divide less frequently and contribute to regenerate all intestinal lineages with slow kinetics. Single cell transcriptomic analysis revealed two classes of Lgr5-high cells, one of them defined by the Mex3a-expression program and by low levels of proliferation genes. Lineage tracing experiments show that large fraction of Mex3a+ cell population is continuously recalled into the rapidly dividing self-renewing ISC pool in homeostatic conditions. Chemotherapy and radiation target preferentially rapidly dividing Lgr5+ cells but spare the Mex3a-high/Lgr5+ population, which helps sustain the renewal of the intestinal epithelium during treatment.

Correspondence should be addressed to: Eduard Batlle (eduard.batlle@irbbarcelona.org).

Author Contributions

F.M.B. and E.B conceived the project. F.M.B. designed and characterized the Mex3a$^{Tom\text{-}creERT2}$ allele, performed FACS, histology and expression analysis of the different mouse models and analyzed results. E.M. performed organoid growth assays and histology experiments. X.H.M performed mouse handling and in vivo experimental manipulations. C.S.A. developed the biostatistical pipeline and methods to analyze single cell data. M.S. performed histology experiments. H.H, I.G, M.G, A.G-A and G.R-E performed library preparation, sequencing and transcript mapping in single cell transcriptomic analysis. M.N. and O.Y performed RNAscope ISH. S.A.J. B. and D.J.W. provided the Cyp1a1::H2B-YFP mouse model. E.B. supervised the project, analyzed results, and wrote the manuscript with the assistance of F.M.B.

INTRODUCTION

The small intestine is the fastest self-renewing tissue in mammals (Clevers, 2013). Cells are generated within invaginations of the epithelium called crypts, migrate rapidly towards the surface and die at the tip of finger-like protrusions known as villus. This whole process takes less than a week. In homeostasis, cell loss in the villus is compensated by continuous cell production in crypts. The rapid cellular turnover of the intestine is powered by Lgr5+ intestinal stem cells (ISCs) that reside at the bottommost positions of the crypts (Barker et al., 2007). Lgr5+ cells actively proliferate and give rise to progenitors that differentiate as they reach the top of the crypts. Large numbers of absorptive cells (enterocytes) and mucosecreting cells (goblet cells) that populate the intestinal epithelium are generated by amplification of the progenitor pool through several rounds of cell division before differentiation. A subset of progenitor cells undergo differentiation to Paneth cells, which remain intermingled with Lgr5+ cells at the base of the crypt. In addition, the small intestine contains three low abundance cell types; Enteroendocrine cells which are hormone secreting cells scattered throughout the crypt and villus, Microfold (M) cells which line the Peyer patches and initiate mucosal immunity and Tuft cells which are dedicated to sense and trigger responses to helminth parasites. Enteroendocrine, M- and Tuft cells in the intestine represent less than 1 epithelial cell in every 100.

Lgr5+ ISCs proliferate as a homogenous cell pool (Snippert et al., 2010), with a rate of about 1 division per day (Barker et al., 2007). Such high proliferation rate, renders Lgr5+ ISCs sensitive to DNA and cytostatic damage (Tao et al., 2015). Despite single cell profiling supported the absence of heterogeneity in Lgr5+ cell population (Grün et al., 2015), the intestine displays a remarkable capacity to recover from these insults, suggesting the existence of reserve or facultative stem cells in a relatively quiescent state. Numerous studies have proposed that quiescent ISCs occupy the +4 crypt position and express markers such as Bmi1, mTert, Lrig1 or Hopx (Montgomery et al., 2010; Powell et al., 2012; Takeda et al., 2011; Yan et al., 2012). Yet, the existence and identity of such quiescent ISCs has been largely controversial (Muñoz et al., 2012) and remains a matter of debate. It was also shown that upon damage of the Lgr5+ pool, committed progenitor cells undergo dedifferentiation and act as facultative stem cells by regenerating the ISC compartment. For example, Alpi1+ enterocytes act as facultative stem cells upon genetic ablation of Lgr5+ cells (Tetteh et al., 2016). Likewise, crypt progenitors that express the Notch ligand Dll1 give rise to secretory cells in homeostatic conditions yet they produce Lgr5+ ISCs upon radiation-induced damage of the intestine (van Es et al., 2012). Secretory cell progenitors are slow proliferating, retain DNA labels and are relatively resistant to chemotherapeutic drugs (Buczacki et al., 2013).

Mex3a belongs to the Mex3 family which in mammals contains four members encoded by different genes: Mex3a, Mex3b, Mex3c and Mex3d. Mex3 proteins have highly conserved RNA binding domains and a C-terminal RING finger domain with E3 ubiquitin ligase activity (Buchet-Poyau et al., 2007). The role of Mex genes in mammals is largely unknown, yet their C. elegans homologue – mex3 -, is required for germline stem cell identity and maintenance (Ciosk et al., 2006) whereas human MEX3A has been correlated to stemness in colon cancer cell lines (Pereira et al., 2013). Here we report that Mex3a labels a subpopulation of slow proliferating progenitor cells located around +3/+4 crypt position. In

homeostatic conditions, Mex3a-high cells give rise to cells that differentiate to all intestinal lineages with low output. A substantial proportion of Mex3a-high cells also produce rapidly proliferating ISCs in homeostasis. Upon damage with chemotherapy or irradiation, Mex3a-high cells are spared and a larger proportion of this population contributes to regenerate the rapidly proliferating ISC pool.

RESULTS

Characterization of Mex3a-expressing intestinal cells

We compared the specific transcriptional programs of ISCs of the mouse small intestine (Muñoz et al., 2012), mouse large intestine and human colon (Jung et al., 2011) (Suppl. Fig 1A. and Table S1). These three sets of ISCs were characterized by expression of canonical intestinal stem cell markers such as Lgr5 (Barker et al., 2007), Ascl2 (van der Flier et al., 2009), EphB3 (Batlle et al., 2002) and Smoc2 (Muñoz et al., 2012). We focused our attention on the RNA binding protein Mex3a, which was enriched in the three types of ISCs yet it had not been previously studied in the intestine. We confirmed by RT-qPCR that Mex3a was upregulated in human and mouse ISCs (Figure 1A). By RNAscope ISH, we found Mex3a mRNA restricted to crypt base columnar cells (CBCs). Many crypts displayed low Mex3a levels yet about half of the crypts in each section contained 1–3 CBCs with relative higher Mex3a mRNA abundance. These Mex3a-high cells were preferentially located at +3/+4 crypt position. (Figure 1B, Figure S1B). To analyze functionally the population of cells that express Mex3a, we generated mice bearing a transcriptional reporter cassette knocked-in at the start codon of Mex3a locus. The reporter cassette consisted in tdTomato and CreERT2 cDNAs separated by self-cleavage T2A peptide (Figure 1C, Figure S1C). We termed this mouse strain $Mex3a^{Tom\text{-}CreERt2/+}$ (from now on referred to as $Mex3a^{Tom/+}$).

$Mex3a^{Tom/+}$ were born at mendelian ratios, had normal lifespans, were fertile, and showed no overt phenotype. Analysis of reporter expression in the intestine revealed Tomato positive (Tom+) cells positioned at the crypt base. The expression of the reporter was low, which is in agreement with the low endogenous levels of Mex3a mRNA detected by RT qPCR and ISH. The most positive cells were located above (i.e. suprabasal) the uppermost Paneth cell, around position “+3/+4” of the crypt (Figure 1C), which is in agreement with the expression of endogenous Mex3a. Tom-high cells comprised around 1 % of the total population of crypt-enriched epithelial cells of the small intestine shown by flow cytometry of dissociated intestines (Figure 1D), thus suggesting that each crypt contains 2–3 Mex3a-high cells and about 4–9 Mex3a low cells, which is in accordance with the ISH data. We next isolated by FACS epithelial cells displaying high, low or negative levels of the Tomato reporter and analyzed expression of known key intestinal marker genes (Figure 1E–G). This experiment demonstrated that Tomato brightness reported Mex3a mRNA levels (Figure 1E). Genes driven by WNT signaling in ISCs such as Lgr5, Ascl2, Axin2, Fzd2 or Smoc2 were expressed at similar levels in Mex3a-high compared to Mex3a-low cells whereas Mex3a-neg cells displayed several fold lower expression (Figure 1E). In contrast, expression of markers of mucosecreting and enterocyte differentiation was highest in the Mex3a-negative cell population (Figure 1F). We also assessed the levels of putative +4 ISC markers. We observed

a small yet consistent enrichment in Bmi1 and Tert in Mex3a-high cells (Figure 1G). To further define the phenotype of Mex3a-expressing cell populations, we performed transcriptomics of Mex3a-high, -low and –neg cells (Table S2). Gene ontology analysis showed that Mex3a-high cells were enriched in genes encoding secretory cell functions, hormone metabolic processes and also in genes that regulate negatively the cell cycle (Figure 1H, Table S3). This profile differed substantially from that of Lgr5-high cells, which were characterized by expression of genes that promote mitosis, Wnt signaling and biosynthetic processes as previously reported (Figure 1H, Table S3)(Muñoz et al., 2012).

Mex3a-high cells are slow proliferating

In agreement with the expression of a gene program of negative regulation of cell proliferation in Mex3a-high cells, we confirmed high levels of the cyclin-dependent kinase inhibitors p57 (Cdkn1c) and p21 (Cdkn1a) in Mex3a-high cells (Figure 2A). To study the proliferative status of Mex3a-expressing cells in vivo, we interrogated Cyp1a1::H2B-YFP mice which express H2B-YFP under the control of the beta-naphthoflavone-inducible Cyp1a1 promoter in all epithelial intestinal cells except for Paneth cells. In pulse-chase experiments, only long-lived slow proliferating cells retain the H2B-YFP label after 10 days of induction with beta-napthoflavone (Buczacki et al., 2013). Label-retaining cells (LRCs) were characterized by elevated levels of both Mex3a and Lgr5 (Figure 2B). Analysis of the transcriptomes of LRCs revealed 68 genes specifically upregulated in LRCs (H2B-YFP+ compared to H2B-YFP- cells and to Paneth cells, Table S4). This LRC signature was very significantly enriched in Mex3a-high cells (Figure 2C). We confirmed expression of LRC-specific genes such as Rfx6 and Peg3 by RT-qPCR in Mex3a-high cells (Figure 2D).

To functionally validate the association of Mex3a-high cells with LRCs, we crossed Cyp1a1::H2B-YFP mice with $Mex3a^{Tom/+}$ mice and analyzed the distribution of the two reporters in compound mice. We had previously demonstrated that high surface abundance of the receptor tyrosine kinase EphB2 identify cells at the bottommost positions of the crypt and enable the isolation of ISCs from mouse and human intestine (Jung et al., 2011; Merlos-Suárez et al., 2011). Pulse chase-experiments demonstrated that Mex3a-high/EphB2-high cells retained H2B-YFP compared to the Mex3a-neg/EphB2-high cell population (Figure 2E, 2F). Within H2B-YFP retaining cells, LRC gene expression was largely restricted to the Mex3a-high population (Figure S2A). We also performed classical labeling of proliferative cells using the nucleotide analogue EdU (Figure 2G). These experiments confirmed that Mex3a-high cells retained about 15 fold more EdU than Mex3a-neg cells 10 days after labeling (Figure 2H). From these experiments, we concluded that Mex3a marks a population of slow proliferating cells within the crypt base.

Lineage tracing from Mex3a-high cells

We next sought to analyze the contribution of Mex3a-high cells to intestinal homeostasis (Figure 3). To this end, we crossed $Mex3a^{Tom/+}$ mice to Rosa26 mTmG mice (Muzumdar et al., 2007). In this mouse model, induction with tamoxifen switches on the activity of Mex3a-driven CreERT2, which in turn activates the expression of membrane bound GFP (GFP) in Mex3a-expressing cells and their progeny. In parallel, we analyzed the dynamics of Lgr5+ cells using $Lgr5^{GFP/+}$; $Rosa26R^{LacZ}$ mice (Figure S3A). These experiments were performed

in conditions that trigger recombination in one cell per crypt. We first established the initial position of Mex3a-derived clones. 36 hours after induction, around 80% of clones were located above the uppermost Paneth cells, around the crypt +3/+4 position. Lineage tracing from the $Lgr5^{GFP/+}$ mice showed a distribution of labeled cells complementary to that observed in $Mex3a^{Tom/+}$ mice at this early time point, i.e. 80% of LacZ+ cells were positioned at the crypt base whereas the rest marked +3/+4 crypt cells (Figure 3A) which is also in agreement with previous reports (Barker et al., 2007). The initial position of Mex3a+ clones coincided approximately with that of cells expressing highest levels of Mex3a mRNA by ISH (Figure 1B) and of tdTomato reporter (Figure 1C). However, we could only find about 1 recombined (GFP+) cell every 500 crypts and this frequency remained in a similar range over the first month of tracing despite the progressive increase in clone size (Figure 3B). Thus, recombination of the Rosa26 mTmG reporter allele only occurred in a small fraction of Tomato-CreERt2 expressing cells, which probably reflects poor Cre recombinase activity as a result of low expression of the Mex3a locus. Nevertheless, we confirmed that creERT2 mRNA was largely restricted to Mex3a-high cells (Figure S3B) implying that most traces originate from this population. We also found that clones arising 3 days post tamoxifen, which were mostly composed of one or two cells, retained higher levels of Mex3a and P57 mRNA compared to non-recombined cells (Fig S3C). To avoid biases imposed by this limitation, we assessed a large number of clones for each time point in subsequent experiments (n=56–331 clones per timepoint; Figure 3B).

Clones generated by Mex3a+ cells increased progressively in size yet displayed slow growth kinetics compared to those produced by Lgr5+ cells (Figure 3C–D). At 3 days of tracing around 80% of GFP+ clones in $Mex3a^{Tom/+}$ mice appeared as one or two labeled cells around crypt position +3/+4 (Figure 3C, 3F). At 7 days, approximately 50% of clones were still composed of 1 or 2 cells whereas only one third had expanded beyond 20 cells (Figure 3C Figure 3G). At this time point, most clones within crypts still localized at +3/+4 position (Figure S3D). In contrast, Lgr5+ cells generated clones that after 7 days appeared as ribbons of cells that expanded from the crypt base up to the villus tip (Figure 3D and examples in Figure 3H). This pattern is generated by the rapid proliferation of ISCs as described elsewhere (REF – barker, winton). Importantly, we did not observe a single ribbon in $Mex3a^{Tom/+}$ mice at 7 days of tracing implying that we did not initially mark any fast dividing ISCs. However, ribbons equivalent to those observed in $Lgr5^{GFP/+}$ mice appeared after 14 days of tamoxifen induction and progressively became more abundant up to the point that they were the only clone type present at 28 days (Figure 3C, 3H). Quantification of clone number per crypt indicated that frequency decreased progressively until day 28 to then stabilize coinciding with the preponderance of ribbons clones (Figure 3B). Analysis of clone position over time in $Mex3a^{Tom/+}$ mice showed that the majority migrated into the villus over a period of two weeks yet some clones remained in the crypt even after 14 days (Figure 3E). These delayed clones may result from either slow cell migration or simply represent new clones generated by traced Mex3a+ cells. Altogether, these observations suggest that Mex3a labels a population of slow dividing progenitor cells. A fraction of Mex3a+ cells or of their progeny will give rise to ISCs after approximately 2 weeks.

We next studied the cell composition of the clones formed by Mex3a+ cells. At 3 days post-induction, all single cells and small clones were located around the +3/+4 crypt position and

lacked expression of differentiation markers (Figure 4A). At 1 week, 60 % of clones had migrated into the upper region of the crypt and the villus (Figure 3E). Clones formed by 1 or 2 cells expressed Dclk1, Chga or ANPEP implying differentiation towards tuft, enteroendocrine or adsorptive lineages respectively (Figure 4B). Larger clones (2–20 cells) were composed of both absorptive (Anpep+) and mucosecreting cells (Muc2+) (Figure 4C). We also observed 6 clones out of 241 that were single Paneth cells at the crypt base. Quantification revealed approximately a 3:1 ratio of absorptive versus secretory cell differentiation (Figure 4D). The remaining clones that were located near the crypt base did not express differentiation makers (examples in Fig 4E). We conclude that similarly to Lgr5+ ISCs, Mex3a-high cells generate multilineage progeny yet with low output.

Mex3a is expressed in a subset of Lgr5+ cells

To explore the relationship between Mex3a+ and Lgr5+ cell populations, we crossed $Mex3a^{Tom/+}$ mice with the $Lgr5^{GFP/+}$ strain (Barker et al., 2007) and analyzed the distribution of the two fluorescent reporters in crypt cells. Previous studies had shown that Lgr5-high cells represent ISCs whereas Lgr5-low cells are early transient amplifying cells (van der Flier et al., 2009). GFP-negative cells are not informative of Lgr5 mRNA as a result of mosaicism in transgene expression in these mice (Schuijers et al., 2014). We thus limited our analyses to the distribution of Mex3a-Tomato within the Lgr5-GFP+ gate. Lgr5-high/Mex3a-high cells represented around 5% of total GFP cells and Lgr5-low/Mex3a-high cell represented around 4% of total GFP cells. (Figure 5A, Figure S5A). Thus, Mex3a-high cells represent 1 in every 5 Lgr5-high and 1 in every 16 Lgr5 low cells respectively.

We measured expression of marker genes by RT-qPCR across the 6 cell populations defined by Mex3a-Tomato and Lgr5-GFP levels (Figure 5B–F and Table S5). ISC-specific and WNT-driven genes were elevated in Lgr5-high cells regardless of Mex3a expression. Mex3a mRNAs were highest in Mex3a-high/Lgr5-high cells (Figure 5B). Paneth cell-specific genes such as Defa and Lyz1 were expressed in Mex3a-high/Lgr5-high cells (Figure 5D) yet levels of these genes were 80 fold lower in Mex3a-high cells than in mature Paneth cells (Figure S5C). Consistent with our previous data, Mex3a-high cell populations contained 2–3-fold more Bmi1 mRNA (Figure S5B).

The Lgr5-low cell population was characterized by reduced expression of ISC/WNT genes and elevated levels of markers of intestinal differentiation as previously reported (Figure 5B–C)(van der Flier et al., 2009). Mucosecreting (Muc2+/Tff3+) and absorptive progenitor cells (Alpi+) were captured in Lgr5-low/Mex3a-low and Lgr5-low/Mex3a-neg gates implying that these cells represent transient amplifying cells (Figure 5C). Dll1+ a marker of secretory precursors, was in the limit of detection yet it did not show differential expression between subpopulations (Figure S5B). Interestingly, Lgr5-low/Mex3a-high cell population expressed genes characteristic of low abundant lineages; tuft cells (Dclk1), enteroendocrine cells (Chga) and M cells (Spib) (Figure 5D). Altogether, these expression patterns indicate that Mex3a-high/Lgr5-high cells resemble ISCs with an incipient expression of genes characteristic of both Paneth and rare secretory cells. Of note, most of the clones observed in lineage tracing experiments using the $Mex3a^{Tom}$ driver probably originated from this cell

population as inferred from the observation that they expressed highest levels of CreERT2 (Figure 5B).

We next assessed the clonogenic potential of Mex3a/Lgr5 subpopulations using as readout their ability to form *in vitro* organoids (Sato et al., 2009). As previously reported, Lgr5-high cells showed highest organoid forming capacity in media supplemented with RSPON1, EGF and NOGGIN (REF). We found, however, that Mex3a-high/Lgr5-high formed 3-fold and 10-fold more organoids than Mex3a-Low/Lgr5-high and Mex3a-neg/Lgr5-high cell populations respectively (Figure 5E, 5F). Organoids generated from Mex3a-high/Lgr5-high cells contained all intestinal lineages (Figure 5G) and could be maintained during multiple passages (n=8) implying self-renewal and multilineage differentiation potential. Finally, to test whether Mex3a-high/Lgr5-Low cells could gain clonogenic potential under conditions that promote self-renewal, we enforced WNT and NOTCH signaling using CHIR99021 and valproic acid, two small molecules that maximize signaling from these pathways in the absence of ligands (Yin et al., 2014). In these conditions, cells remain blocked in an ISC-like state as indicated by the formation of spheroids yet Mex3a-high/Lgr5-Low and Mex3a-low/Lgr5-Low remained poorly clonogenic (Figure S5D,).

Single cell transcriptomics identifies a subpopulation of Lgr5-high cells enriched in the Mex3a signature

The finding that a subset of Lgr5-high cells expresses Mex3a and that Mex3a-high/Lgr5-high display slow proliferation kinetics implies heterogeneity of ISC pool. This finding is in sharp contrast with recent single cell transcriptomic analysis of Lgr5-high cells performed by Grün et al (REF), which conclude that this population is largely homogenous (REF). Indeed, we reanalyzed the Grün dataset and failed to identify an obvious Lgr5+ subpopulation expressing the Mex3a-specific signature. We, however, reasoned that this negative result might simply be due to underrepresentation of the Mex3a population as the Grün dataset contained sequences of only 53 individual cells at a relatively low coverage (0.4 million reads per cell). Therefore, we set out to generate transcriptomic data for a larger number of Lgr5-high cells at a higher sequencing depth. To this end, the top 25% of brightest Lgr5-GFP+ cells from the small intestine were isolated and loaded into a microfluidic chip. We performed full transcriptomic profiles by RNA Seq of 400 capture sites. Subsequently, we removed both empty captured sites and those sites that contained visually identified cell doublets. Additionally, we applied stringent filters to further discard cells displaying either very low transcript counts or cells with transcript distributions that scored with elevated probability of belonging to cell aggregates (see methods for details). The final high-quality dataset contained 245 individual Lgr5-high cells sequenced at an average of 1.8 million reads per cell (Figure 6A). We computed unique molecular identifiers (UMIs) and assessed cell population distribution using principal component analysis (PCA). These analyses grouped Lgr5-high cells into two well-defined clusters. Cluster 1 and cluster 2 contained 140 and 105 cells Lgr5-high cells respectively (Figure 6B). Optimal cluster number was not affected by coverage as shown by downsampling analysis (Figure S6A), yet a reduction of cell numbers below 50% precluded the identification of the two Lgr5-high cell populations (Figure S6B). We estimated that the classification (out-of-bag) error of cells into the two predefined cell clusters using the downsampled datasets was stable around 10%

but it increased if using either less than 20% of cells or sequencing reads (Figure S6C, S6D). Thus, a minimal number of cells with sufficient coverage are required to identify these two Lgr5-high clusters.

The ISC-specific genes Lgr5, Smoc2, Olfm4 and Axin2 were expressed at equal levels in cluster 1 and 2 (Figure 6C). Furthermore, the average level of the Lgr5-GFP-high specific gene expression signature was equivalent in the two clusters. Therefore, both cluster 1 and 2 contain bonafide Lgr5-high cells (Figure 6D). Lowly expressed genes such as Mex3a, Tert or Dll1 were captured with very low coverage in our dataset (i.e. an average of X UMI per cell), which precluded reaching reliable conclusions about their expression pattern. However, we found that the Mex3a-high signature was largely upregulated in cells belonging to cluster 2 (Figure 6E). Furthermore, those genes upregulated in Mex3a-high/Lgr5-high cells compared to Mex3a-neg/Lgr5-high cells were enriched in cluster 2 (Table S6 and Figure S6E). There was no correlation between expression of Lgr5-high and Mex3a-high signatures (Figure 6F).

The above data imply that cluster 2 contains Lgr5-high cells that express the gene program characteristic of Mex3a-high cells. However, it was evident from the PCA plots that the Mex3a gene program was expressed in a graded manner; this is, it increased as cells from cluster 2 separate from cluster 1 along PC1 axis. We found that the graded expression of the Mex3a program correlated inversely with a signature characteristic of Ki67+ crypt cells obtained from Ki67-RFP knock-in mice (Figure 6G, 6H, REF Basak) which is enriched in genes required for mitosis and progression through the cell cycle (Table S6). Therefore, as Lgr5-high cells become progressively Mex3a positive they lower expression of the proliferation program.

Finally, a recent study has identified a subset of Lgr5-high cells characterized by incipient expression of makers of both of absorptive and secretory lineages. It was proposed that these “primed” Lgr5-high cells, termed intestinal bipotent progenitors (IBPs), may represent ISCs undertaking the first step toward differentiation before commitment to either lineage (Kim et al., 2016). We used genes enriched in IBPs to identify this population in our dataset and confirmed that a fraction of Lgr5-high cells expressed markers of both absorptive and secretory lineages. IBP-like cells were present in both cluster 1 and 2 and therefore they did not represent a main source of cell heterogeneity in the PCA analyses (Figure S6F).

Mex3a-expressing cells are resistant to both chemotherapy and γ-radiation

Standard chemotherapy and γ-radiation treatments are aimed at killing rapidly dividing cells. A main example is 5-Fluorouracil (5FU), which blocks thymidine synthesis thus impeding DNA replication. γ-radiation induces double strand breaks in all cell types, albeit with higher toxicity in highly proliferative cells. Consistent with this notion, treatment of mice with both high dose 5FU and IR reduced significantly the Lgr5-high cell population (Figure 7A, 7B, Figure S7A, S7B). In contrast, the frequency of Mex3a-high cells increased upon treatment (Figure 7A, 7B, Figure S7A, S7B). Analysis of compound $Mex3a^{Tom/+};Lgr5^{GFP/+}$ mice showed that Mex3a-high/Lgr5-high cells were more resistant to 5-FU and IR than Lgr5-high/Mex3a-low and Lgr5-high/Mex3a-neg cells (Figure 7C, 7D). Mex3a expression also segregated Lgr5-low cells according to their sensitivity to 5-FU and

IR. Lgr5-low/Mex3a-neg cells, which represent the bulk of the transient amplifying compartment, were highly sensitive to these insults whereas the relative numbers of Lgr5-low/Mex3a-high and Lgr5-low/Mex3a-low cells increased upon treatment (Figure 7C, 7E). Therefore, the majority of Lgr5-high and Lgr5-low cells that resisted 5FU expressed Mex3a. As we assessed cell numbers 48 hours after treatment, the observed frequencies likely reflect relative survival rates rather than proliferation and subsequent expansions of each subpopulation.

We next studied the contribution of Mex3a-high cells to tissue renewal upon chemotherapy by mapping their fate using lineage tracing analysis. We did not find significant differences in clone size or numbers at early time points of treatment (Figure S7C, S7D). Importantly, 1 week after 5FU treatment, Mex3a+ cells produced larger clones, including 10% of ribbons that were never present in untreated mice at this time point (Figure 7F, 7G). All clones produced in control or 5FU-treated $Mex3a^{Tom/+}$ mice arose from +3/+4 crypt position, except for ribbons that started at the crypt base (Figure S7E). Two weeks after 5FU treatment, the percentage of crypt base-to-villus ribbons generated by Mex3a-high cells increased by over two fold compared to controls (Figure 7G). These patterns fit well with the notion that Mex3a-high cells are not only relatively resistant to chemotherapy but also contribute to regenerate the rapidly proliferating ISC pool after damage.

DISCUSSION

The features and behavior of Mex3a+ cells are unique among other previously characterized crypt cell populations. Mex3a-high cells resemble Lgr5+ crypt base columnar cells in that they express high levels of WNT-driven ISC-specific genes. However, the progeny of Mex3a-high cells originates largely from +3/+4 position and is substantially less abundant than that produced by bulk Lgr5+ cell population during equivalent periods. Mex3a+ cells generate multilineage progeny and therefore they neither represent progenitor committed to particular lineages. Dll1, Dclk1, Ngn3 or Alpi mark short-lived progenitor cells that differentiate towards particular lineages (Nakanishi et al., 2013; van Es et al., 2012; Wang et al., 2007). None of these populations contribute long-term to renewal of the epithelium in homeostatic conditions. In contrast, a large fraction of Mex3a population is recalled to the ISC pool and regenerates the epithelium over months.

Mex3a-high cells display features reminiscent of crypt Label Retaining Cells (LRCs) originally identified by Chris Potten (Potten et al., 1978) and later characterized by the Winton lab (Buczacki et al., 2013). The observation that the H2B-YFP mark that accumulates in LRCs is inherited by enteroendocrine and Paneth cells led to the proposal that these cells are precursors of these secretory lienages (Buczacki et al., 2013). Experiments of lineage-tracing using a bipartite Cre recombinase in which the enzyme is reconstituted only in label retaining cells indicated that this cell population does not retain clonogenic capacity in homeostasis (Buczacki et al., 2013). Similarly to LRCs, Mex3a-high cells accumulate nucleotide analogues as a result of their low proliferation rates and display incipient expression of Paneth Cell markers. Yet, Mex3a-derived clones contain larger proportion of absorptive cells, which reflect the greater abundance of this cell type in the small intestine, and therefore Mex3a+ progeny is not biased towards the secretory lineage.

More importantly, unlike LRCs described in (Buczacki et al., 2013), Mex3a-high cells or its progeny produce ribbon clones in homeostatic conditions implying long-term clonogenic potential. The reasons for the discrepancy between the behavior of H2B-YFP-retaining cells reported in the previous study (Buczacki et al., 2013) and that of the Mex3a-high cells described herein are unclear but indicate that these two populations are not completely overlapping. A potential cofounding effect is the fact that Mex3a-high cells include both Lgr5-high and Lgr5-low populations. Mex3a-high/Lgr5-high cells express the ISC/WNT program and are highly clonogenic ex vivo. In contrast, Mex3a-high/lgr5-low cells are characterized by higher levels of enteroendocrine and tuft cell genes and give rise organoids with very low efficiency. We thus speculate that lineage tracing from the bipartite cre/H2B present in the previous study (Buczacki et al., 2013) may largely reflect the behavior of the Mex3a-high/Lgr5-low population. Testing this hypothesis will require generation of genetic tools that enable fate mapping from each of these two populations.

Single cell transcriptomic analysis revealed previously unanticipated heterogeneity of Lgr5-high cells and provided evidence for the existence of two phenotypes within this cell population. Both classes of Lgr5-high cells are marked by genes that define canonical ISCs. Additionally, cells in cluster 2 express the gene program of Mex3a+ cells. The average expression of Mex3a signature is anti-correlated with that of Ki67+ progenitor cells, an observation that fits in well with the limited cellular output generated by Mex3a+ cells in lineage tracing experiments. The graded levels of Mex3a-specific gene signature across cluster 2 cells suggest that some cluster 1 cells may progressively acquire this phenotype. Lgr5-driven creERT2 marks both cluster 1 and cluster 2 cells and therefore this tracer is not useful to test this hypothesis.

Our data indicate that Mex3a-high/Lgr5-high cells represent a subset of ISCs undergoing a state of relative quiescence. Given their low division rate, Mex3a-high cells have a modest contribution to sustain renewal of the epithelium under homeostatic conditions. According to the lineage tracing experiments, individual cells and small clones derived from Mex3a-high cells last for about two to three weeks suggesting that this is the approximate life-span of the Mex3a-high cell population. This data fits in well with the possibility that slow proliferating Mex3a-high cells are continuously displaced by the rapidly dividing ISCs as a result of the neutral competition dynamics that drive renewal of the intestinal epithelium (Snippert et al., 2010). An alternative explanation for the long residence time of Mex3a-derived clones in crypts would be that over a period of two weeks, Mex3a+ cells keep producing new progeny, which is observed as individual cells or small cell clones in each experimental time point. Importantly, a fraction of Mex3a-derived cells are converted to rapidly proliferating ISCs as shown by the emergence of crypt base-to-villus clones (“ribbons”) in two weeks tracing experiments. The fact that we never observed ribbon-like clones before this period implies that Mex3a-driven creERT2 does not initially mark fast dividing ISCs.

Finally, Mex3a cells are largely resistant to cytotoxic stress such as chemotherapy and radiotherapy when compared to bulk Lgr5+ ISCs (Tao et al., 2015). This property is likely the consequence of their relative slow proliferation rates. Upon 5FU treatment, the rate of conversion of Mex3a-high cells to ISCs is exacerbated. Mounting evidence indicates that Dll1+ secretory progenitors (van Es et al., 2012) and even differentiated enterocytes (Tetteh

et al., 2016) exhibit plasticity and regain stemness upon depletion of the Lgr5+ pool. We argue that reversion of differentiated cells to a stem cell state is probably a rare event that does not contribute substantially to regenerate the epithelium after chemotherapy or radiation. Indeed, De Sauvage and colleagues demonstrated that Lgr5+ cell population is necessary to regenerate the epithelium upon irradiation (REF). Our experiments show that chemotherapy and radiation eliminates preferentially Lgr5-low/Mex3-low cell population, which contains the bulk of transient amplifying cells in the crypt. In contrast, Mex3a+ cell population continues to generate progeny immediately after 5FU treatment. In these conditions, about 40% of Mex3a-high cells produce ribbon-like clones implying that a large proportion contribute to generate the compartment of fast dividing Lgr5+ ISCs. Given the fact that Mex3a-high/Lgr5-low cells show little clonogenic capacity in *ex vivo* assays, we favor the idea that resilient Mex3a-high/Lgr5-high cells contribute the most to regeneration after damage. Therefore Mex3a-high cells represent a reservoir of slow-dividing chemotherapy- and radiotherapy-resistant Lgr5+ cells.

EXPERIMENTAL PROCEDURES

Analysis of ISC signatures

To identify robust ISC genes we compared three lists of candidate ISC genes derived from expression signatures of mouse and small intestine populations. To this end, we overlapped the expression profile of small intestine Lgr5 cells (Muñoz et al., 2012) with the previously characterized human EPHB2 derived signature (Jung et al., 2011), and a signature derived from mouse colon Lgr5 cells (see below).

Generation of the Mex3a reporter allele

A cassette bearing a tdTomato/T2A/Cre-ERT2/bGH polyA was inserted in frame with the Mex3a start codon in exon 1. Detailed protocols are provided in Supplemental information.

Mouse models

Lgr5::EGFP-IRES-Cre-ERT2 mice were obtained from the laboratory of Dr. Hans Clevers. Cyp1a1::H2B-YFP mice were obtained from the laboratory of Dr. Douglas J. Winton. Mice were housed and bred according to IRB Barcelona and PCB institutional guidelines.

Treatments

Cyp1a1::H2B-YFP model: For the induction of the Cyp1a1::H2B-YFP allele, mice were given 3 intraperitoneal doses of β-napthoflavone (80 mg/kg, Sigma) over a 36 hour period and followed as previously described (Buczacki et al., 2013).

Lineage tracing—For lineage tracing experiments in the Mex3aTom/+ model, mice were injected with two consecutive intraperitoneal doses of tamoxifen (20 mg/kg, Sigma). For early time points (i.e. 36 hours), mice were treated with a single dose of 4-OH tamoxifen (5 mg/kg, Sigma). The efficiency of the Mex3a-driven creERT2 was 1 recombination event per 500 crypts, which rendered all Mex3a tracing experiments to be in single cell recombination conditions. For lineage tracing from the $Lgr5^{GFP/+}$ model, 1 dose of diluted Tamoxifen (2 mg/kg) was used to ensure tracing from single cell conditions.

Label retention assay—For EdU label-retention, Mex3a$^{Tom/+}$ mice were treated with 3 intraperitoneal doses (1 mg/25 g, Life technologies) in a 36 hour period and analyzed 10 days after the final dose.

5-FU and IR treatments—Damage to the intestinal epithelium was done by injecting two intraperitoneal doses of 5-fluorouracil (100 mg/kg, Sigma) or 12 Gy. For lineage tracing experiments mice were injected with tamoxifen, treated with 5-FU and analyzed at 3, 7 or 15 days after the first dose of tamoxifen.

Intestinal crypt cell purification and staining

Intestinal crypt cells were purified as previously described (Merlos-Suárez et al., 2011). Detailed protocols are provided in Supplemental information.

Transcriptomics, GO and GSEA analysis

Detailed protocols are provided in Supplemental information.

Tissue staining

Detailed protocols for Immunohistochemistry, in situ hybridization, and immunofluorescence are provided in Supplemental Information.

Single cell transcriptomics

Detailed protocols are provided in Supplemental information.

Supplementary Material

Refer to Web version on PubMed Central for supplementary material.

Acknowledgments

We thank Elena Sancho, Anna Merlos-Suárez, Andreu Casali, Peter Jung, Travis H. Stracker and Alexandra Avgustinova for helpful discussions. We thank all members of the Batlle laboratory for support and discussions. We are also grateful for the assistance by the IRB Barcelona core facilities for Histopathology, Functional Genomics, Biostatistics, and Advanced Digital Microscopy, as well as the PCB Flow Cytometry platform. This work has been financed by Spanish Ministry of Science and Competitivity (SAF2011-27068). Work in the laboratory of Dr. Batlle is supported by Fundación Botín and Banco Santander, through Santander Universities.

References

Barker N, Bartfeld S, Clevers H. Tissue-resident adult stem cell populations of rapidly self-renewing organs. Cell stem cell. 2010; 7:656–670. [PubMed: 21112561]

Barker N, van Es JH, Kuipers J, Kujala P, van den Born M, Cozijnsen M, Haegebarth A, Korving J, Begthel H, Peters PJ, et al. Identification of stem cells in small intestine and colon by marker gene Lgr5. Nature. 2007; 449:1003–1007. [PubMed: 17934449]

Batlle E, Henderson JT, Beghtel H, Van den Born M, Sancho E, Huls G, Meeldijk J, Robertson J, Van de Wetering M, Pawson T, et al. B-Catenin and TCF Mediate Cell Positioning in the Intestinal Epithelium by Controlling the Expression of EphB/EphrinB. Cell. 2002; 111:251–263. [PubMed: 12408869]

Buczacki SJA, Zecchini HI, Nicholson AM, Russell R, Vermeulen L, Kemp R, Winton DJ. Intestinal label-retaining cells are secretory precursors expressing Lgr5. Nature. 2013; 495:65–69. [PubMed: 23446353]

Buchet-Poyau K, Courchet J, Le Hir H, Seraphin B, Scoazec JY, Duret L, Domon-Dell C, Freund JN, Billaud M. Identification and characterization of human Mex-3 proteins, a novel family of evolutionarily conserved RNA-binding proteins differentially localized to processing bodies. Nucleic acids research. 2007; 35:1289–1300. [PubMed: 17267406]

Ciosk R, DePalma M, Priess JR. Translational regulators maintain totipotency in the Caenorhabditis elegans germline. Science. 2006; 311:851–853. [PubMed: 16469927]

Clevers H. The intestinal crypt, a prototype stem cell compartment. Cell. 2013; 154:274–284. [PubMed: 23870119]

Grün D, Lyubimova A, Kester L, Wiebrands K, Basak O, Sasaki N, Clevers H, van Oudenaarden A. Single-cell messenger RNA sequencing reveals rare intestinal cell types. Nature. 2015; 525:251–255. [PubMed: 26287467]

Jung P, Sato T, Merlos-Suárez A, Barriga FM, Iglesias M, Rossell D, Auer H, Gallardo M, Blasco MA, Sancho E, et al. Isolation and in vitro expansion of human colonic stem cells. Nature medicine. 2011; 17:1225–1227.

Kim TH, Saadatpour A, Guo G, Saxena M, Cavazza A, Desai N, Jadhav U, Jiang L, Rivera MN, Orkin SH, et al. Single-Cell Transcript Profiles Reveal Multilineage Priming in Early Progenitors Derived from Lgr5(+) Intestinal Stem Cells. Cell reports. 2016; 16:2053–2060. [PubMed: 27524622]

Merlos-Suárez A, Barriga Francisco M, Jung P, Iglesias M, Céspedes María V, Rossell D, Sevillano M, Hernando-Momblona X, da Silva-Diz V, Muñoz P, et al. The Intestinal Stem Cell Signature Identifies Colorectal Cancer Stem Cells and Predicts Disease Relapse. Cell stem cell. 2011; 8:511–524. [PubMed: 21419747]

Montgomery RK, Carlone DL, Richmond CA, Farilla L, Kranendonk MEG, Henderson DE, Baffour-Awuah NY, Ambruzs DM, Fogli LK, Algra S, et al. Mouse telomerase reverse transcriptase (mTert) expression marks slowly cycling intestinal stem cells. Proceedings of the National Academy of Sciences. 2010; 108:179–184.

Muñoz J, Stange DE, Schepers AG, van de Wetering M, Koo BK, Itzkovitz S, Volckmann R, Kung KS, Koster J, Radulescu S, et al. The Lgr5 intestinal stem cell signature: robust expression of proposed quiescent '+4' cell markers. The EMBO journal. 2012; 31:3079–3091. [PubMed: 22692129]

Muzumdar MD, Tasic B, Miyamichi K, Li L, Luo L. A global double-fluorescent Cre reporter mouse. Genesis. 2007; 45:593–605. [PubMed: 17868096]

Nakanishi Y, Seno H, Fukuoka A, Ueo T, Yamaga Y, Maruno T, Nakanishi N, Kanda K, Komekado H, Kawada M, et al. Dclk1 distinguishes between tumor and normal stem cells in the intestine. Nature genetics. 2013; 45:98–103. [PubMed: 23202126]

Pereira B, Sousa S, Barros R, Carreto L, Oliveira P, Oliveira C, Chartier NT, Plateroti M, Rouault JP, Freund JN, et al. CDX2 regulation by the RNA-binding protein MEX3A: impact on intestinal differentiation and stemness. Nucleic acids research. 2013; 41:3986–3999. [PubMed: 23408853]

Potten CS, Hume WJ, Reid P, Cairns J. The segregation of DNA in epithelial stem cells. Cell. 1978; 15:899–906. [PubMed: 728994]

Powell AE, Wang Y, Li Y, Poulin EJ, Means AL, Washington MK, Higginbotham JN, Juchheim A, Prasad N, Levy SE, et al. The pan-ErbB negative regulator Lrig1 is an intestinal stem cell marker that functions as a tumor suppressor. Cell. 2012; 149:146–158. [PubMed: 22464327]

Sato T, Vries RG, Snippert HJ, van de Wetering M, Barker N, Stange DE, van Es JH, Abo A, Kujala P, Peters PJ, et al. Single Lgr5 stem cells build crypt-villus structures in vitro without a mesenchymal niche. Nature. 2009; 459:262–265. [PubMed: 19329995]

Schepers AG, Snippert HJ, Stange DE, van den Born M, van Es JH, van de Wetering M, Clevers H. Lineage tracing reveals Lgr5+ stem cell activity in mouse intestinal adenomas. Science. 2012; 337:730–735. [PubMed: 22855427]

Schuijers J, van der Flier Laurens G, van Es J, Clevers H. Robust Cre-Mediated Recombination in Small Intestinal Stem Cells Utilizing the Olfm4 Locus. Stem Cell Reports. 2014; 3:234–241. [PubMed: 25254337]

Snippert HJ, van der Flier LG, Sato T, van Es JH, van den Born M, Kroon-Veenboer C, Barker N, Klein AM, van Rheenen J, Simons BD, et al. Intestinal crypt homeostasis results from neutral

competition between symmetrically dividing Lgr5 stem cells. Cell. 2010; 143:134–144. [PubMed: 20887898]

Takeda N, Jain R, LeBoeuf MR, Wang Q, Lu MM, Epstein JA. Interconversion between intestinal stem cell populations in distinct niches. Science. 2011; 334:1420–1424. [PubMed: 22075725]

Tao S, Tang D, Morita Y, Sperka T, Omrani O, Lechel A, Sakk V, Kraus J, Kestler HA, Kuhl M, et al. Wnt activity and basal niche position sensitize intestinal stem and progenitor cells to DNA damage. The EMBO journal. 2015; 34:624–640. [PubMed: 25609789]

Tetteh, Paul W., Basak, O., Farin, Henner F., Wiebrands, K., Kretzschmar, K., Begthel, H., van den Born, M., Korving, J., de Sauvage, F., van Es, Johan H., et al. Replacement of Lost Lgr5-Positive Stem Cells through Plasticity of Their Enterocyte-Lineage Daughters. Cell stem cell. 2016; 18:203–213. [PubMed: 26831517]

van der Flier LG, van Gijn ME, Hatzis P, Kujala P, Haegebarth A, Stange DE, Begthel H, van den Born M, Guryev V, Oving I, et al. Transcription factor achaete scute-like 2 controls intestinal stem cell fate. Cell. 2009; 136:903–912. [PubMed: 19269367]

van Es JH, Sato T, van de Wetering M, Lyubimova A, Nee AN, Gregorieff A, Sasaki N, Zeinstra L, van den Born M, Korving J, et al. Dll1+ secretory progenitor cells revert to stem cells upon crypt damage. Nature cell biology. 2012; 14:1099–1104. [PubMed: 23000963]

Wang Y, Giel-Moloney M, Rindi G, Leiter AB. Enteroendocrine precursors differentiate independently of Wnt and form serotonin expressing adenomas in response to active beta-catenin. Proceedings of the National Academy of Sciences of the United States of America. 2007; 104:11328–11333. [PubMed: 17592150]

Yan KS, Chia LA, Li X, Ootani A, Su J, Lee JY, Su N, Luo Y, Heilshorn SC, Amieva MR, et al. The intestinal stem cell markers Bmi1 and Lgr5 identify two functionally distinct populations. Proceedings of the National Academy of Sciences of the United States of America. 2012; 109:467–471.

Yin X, Farin HF, van Es JH, Clevers H, Langer R, Karp JM. Niche-independent high-purity cultures of Lgr5+ intestinal stem cells and their progeny. Nature methods. 2014; 11:106–112. [PubMed: 24292484]

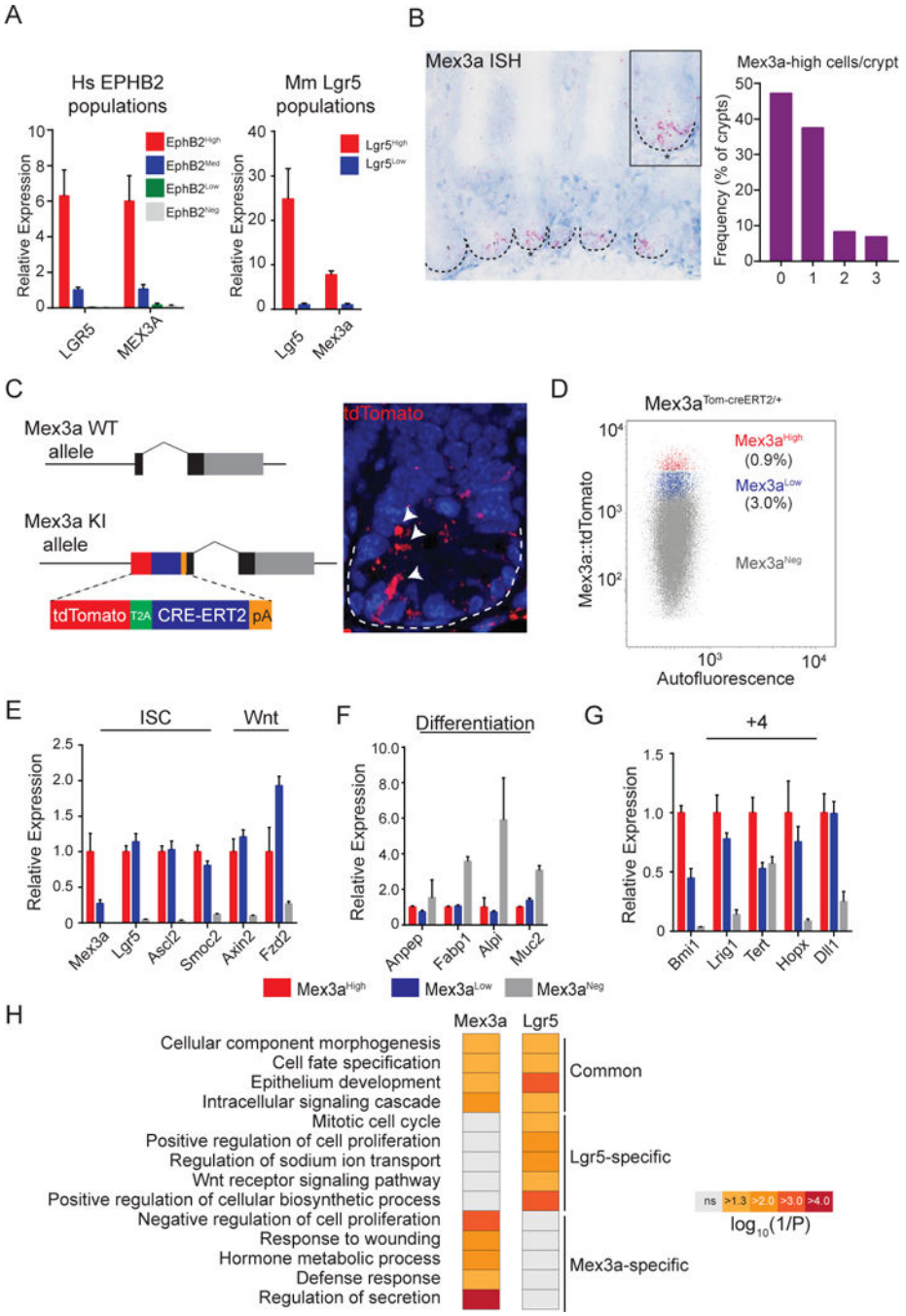

Figure 1. Characterization of the Mex3a reporter allele

(A) Mex3a is enriched in ISC populations. RT qPCR analysis of Mex3a and Lgr5 expression in intestinal populations defined by EPHB2 (left panel) and Lgr5 expression (right panel). Bars depict the mean and upper/lower limits of relative expression obtained from a representative sorting experiment.

(B) Mex3a is expressed at the crypt base and is enriched in suprabasal positions of the crypt. (Left panel) Representative smFISH of Mex3a co-stained for E-Cadherin. (Right panel)

Quantification of Mex3a transcripts by smFISH along the crypt-villus axis. Data represents the mean ± SEM of 25 crypts.

(C) (Left panel) Representation of the Mex3a knock-in allele. A tdTomato/T2A/Cre-ERT2/bGHpolyA cassette was inserted in the translation start site of Mex3a. This construct results in a transcriptional reporter for Mex3a expression driving a tdTomato protein and a tamoxifen inducible Cre recombinase. (Right panel) Immunofluorescence against tdTomato in the small intestine of a $Mex3a^{Tom/+}$ mouse.

(D) Representative FACS profile of a small intestine preparation obtained from a $Mex3a^{Tom/+}$ mouse.

(E – G) Relative expression of known ISC genes (E), differentiation genes (F), and "+4" marker genes (G) in Mex3a populations. Bars depict the mean and upper/lower limits of relative expression determined by RT qPCR obtained from a representative sorting experiment.

(H) Selected GO biological processes enriched in Mex3a and/or Lgr5 signatures. GO category enrichment and statistical analysis was performed using the DAVID Analysis platform.

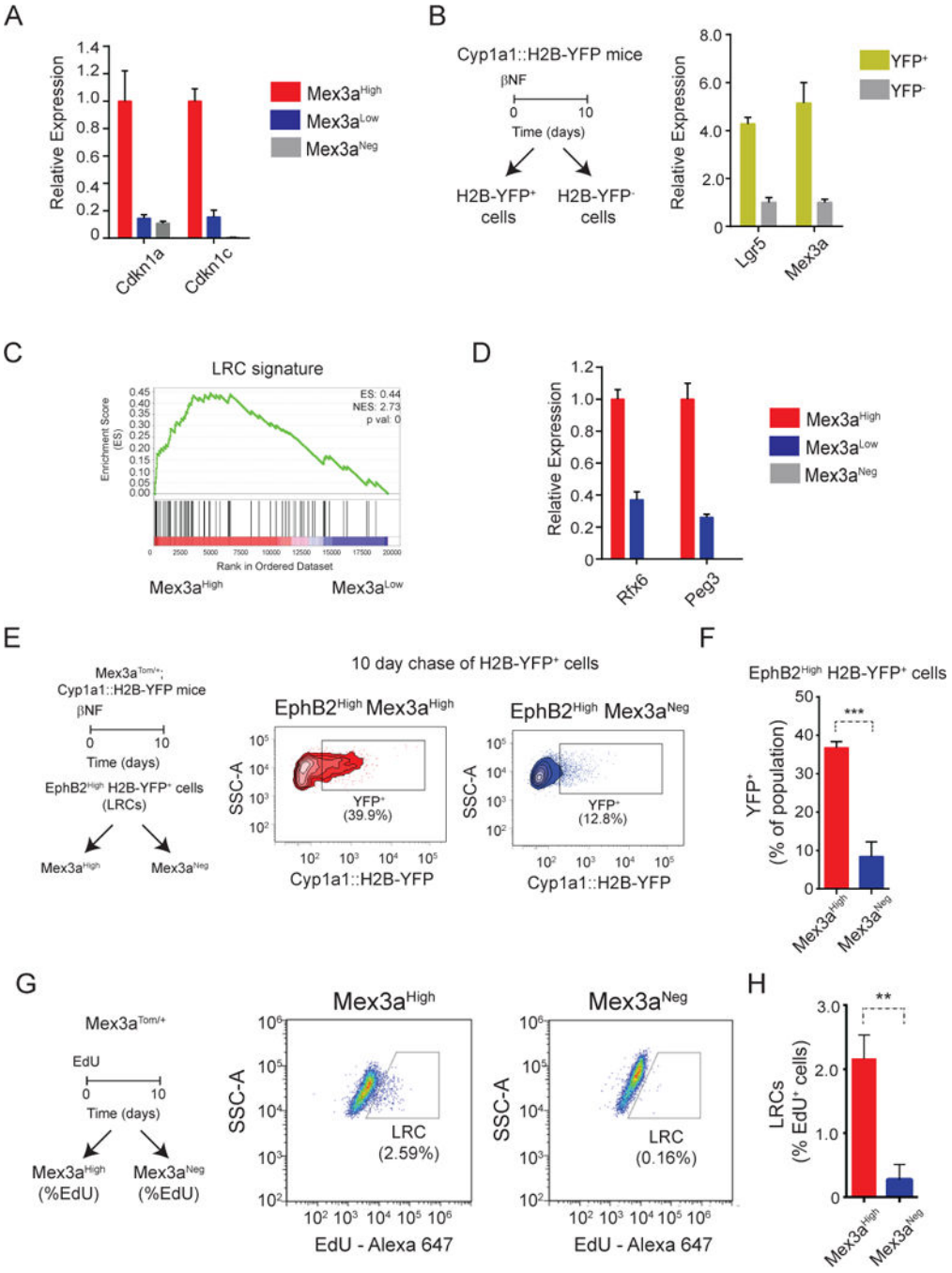

Figure 2. Mex3a expression identifies intestinal label-retaining cells

(A) Mex3a identifies cells with elevated expression of p21 and p57. Expression of cell cycle inhibitors Cdkn1a (p21/WAF1) and Cdkn1c (p57/KIP2) in Mex3a populations. Bars depict the mean and upper/lower limits of relative expression obtained from a representative sorting experiment.

(B) Mex3a is enriched in crypt-base label retaining cells. Lgr5 and Mex3a expression data in label-retaining (YFP+) vs proliferative (YFP-) cells. Bars depict the mean and upper/lower limits from a representative RT qPCR.

(C) GSEA analysis of the previously defined LRC gene expression signature (Table S5) in Mex3a-high vs Mex3a-low cells.

(D) RT qPCR of LRC genes Rfx6 and Peg3 in the Mex3a populations. Bars depict the mean and upper/lower limits of relative expression obtained from a representative sorting experiment.

(E) Experimental protocol. Mex3a/LRC compound reporters were generated and intestinal LRCs were followed by chasing for 10 days after induction. To ensure the analysis of ISC enriched cells, an EphB2 staining was incorporated. Representative FACS plots of LRCs (YFP+) in Mex3a-high and Mex3a-neg cells.

(F) Quantification of the distribution of LRCs in Mex3a-high and Mex3a-neg cells. ***, p value < 0.001 in a two-tailed t-test (n = 3 mice). Bars depict the mean ± SEM.

(G) Experimental design to follow EdU retention. EdU was injected into $Mex3a^{Tom/+}$ mice and 10 days later Mex3a-high and Mex3a-neg cells were sorted and stained for the presence of EdU by FACS. Representative FACS plots of EdU retention in Mex3a-high (Left panel) and Mex3a-neg cells (Right panel).

(H) Quantification of the retention of EdU in Mex3a-high and Mex3a-neg cells. **, p value < 0.01 in a two-tailed t-test (n = 3 mice). Bars depict the mean ± SEM.

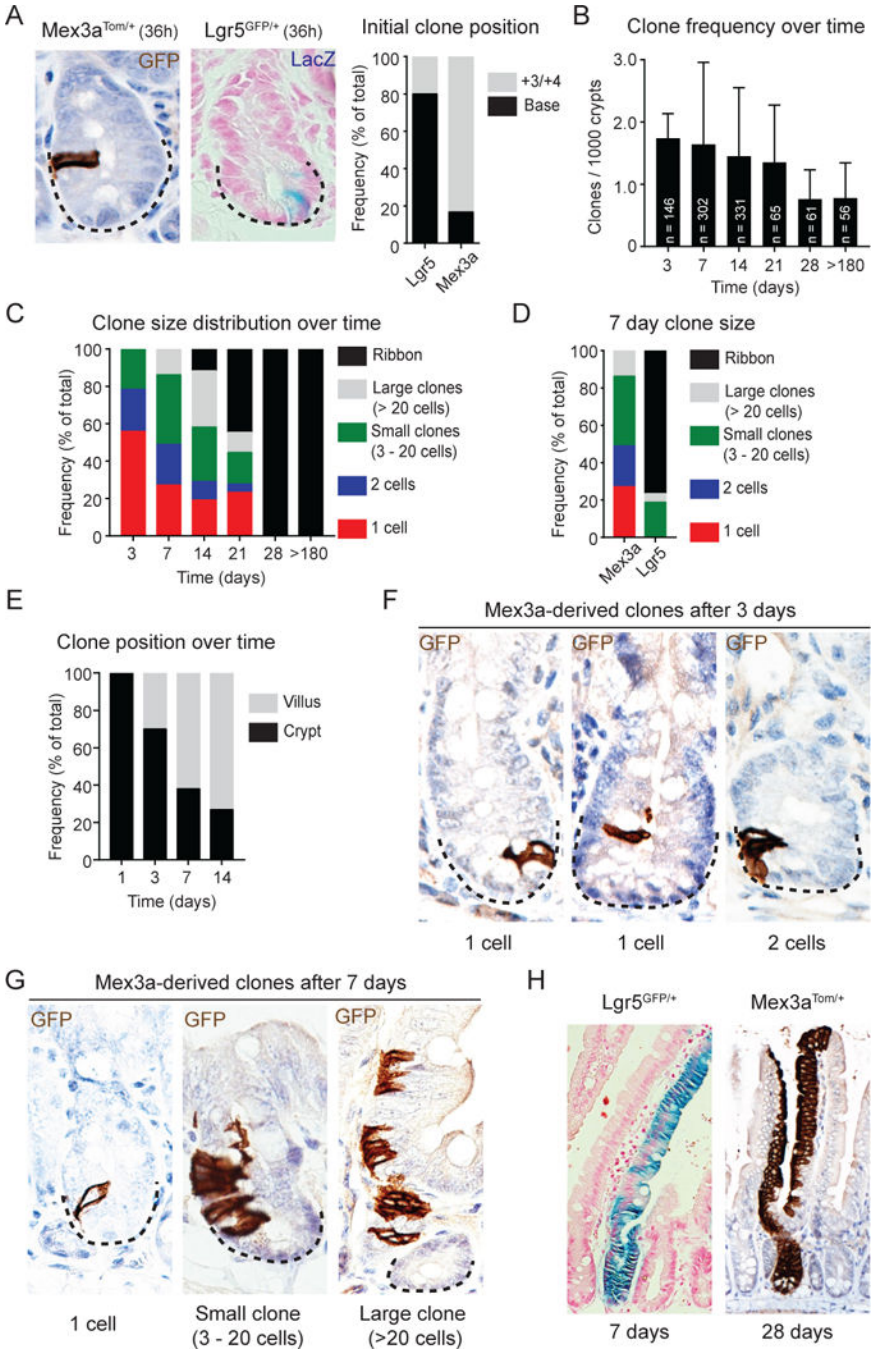

Figure 3. Mex3a-driven lineage tracing

(A) Representative image of a Mex3a GFP+ cell (Left panel) and an Lgr5 LacZ+ cell (middle panel) after 36 hours. (Right panel) Frequency of the position of Lgr5 (Lgr5$^{GFP/+}$) or Mex3a (Mex3a$^{Tom/+}$) labelled cells within the crypt 36 hours after Tamoxifen administration.

(B) Clone frequency over time. Clone frequency per 100 crypts was calculated at 3 days (n = 146 clones), 7 days (n = 302 clones), 14 days (n = 331 clones), 21 days (n = 65 clones), 28

days (n = 61 clones) and over 180 days (n = 56 clones). Data was obtained from at least 15 independent sections from at least 3 mice per time.

(C) Clone size over time. Clone frequency per 100 crypts was calculated at 3 days (n = 146 clones), 7 days (n = 302 clones), 14 days (n = 331 clones), 21 days (n = 65 clones), 28 days (n = 61 clones) and over 180 days (n = 56 clones). Data was obtained from at least 15 independent sections from at least 3 mice per time.

(D) Comparison of clone size distribution at 7 days for Mex3a- (n = 302) and Lgr5- (n = 75) driven lineage tracing.

(E) Analysis of lineage-bias within Mex3a-derived clones. 7 day clones were stained for absorptive and secretory lineage markers to assess their differentiation pattern. (Left panel) 1 and 2 cells clones are largely absorptive, but also secretory cells are found. Single cells remaining at crypts were negative for lineage markers. (Right panel) Clones of over 3 cells are largely undifferentiated after 7 days, yet both lineages are still observed within larger clones.

(F) Mex3a-derived cells rarely incorporate BrdU. 3 day clones (n = 33 clones) were stained for BrdU incorporation.

(G) Characterization of single cell clones after 7 days of tracing. Representative images of single cells stained for GFP+/Dclk1+ cell (left panel) and GFP+/Chga+ (right panel). Arrowheads point to positive cells.

(H) Characterization of large clones after 7 days of tracing. A clone of GFP+/UEA-Lectin+ Paneth cells within a crypt (left panel). Representative image of GFP+/Muc2+ (middle panel) and GFP+/Anpep+ (right panel). White arrowheads point towards positive cells for the lineage marker. Red arrows point to GFP+ cells negative for the stained marker, thus showing that clones are composed by more than a single lineage.

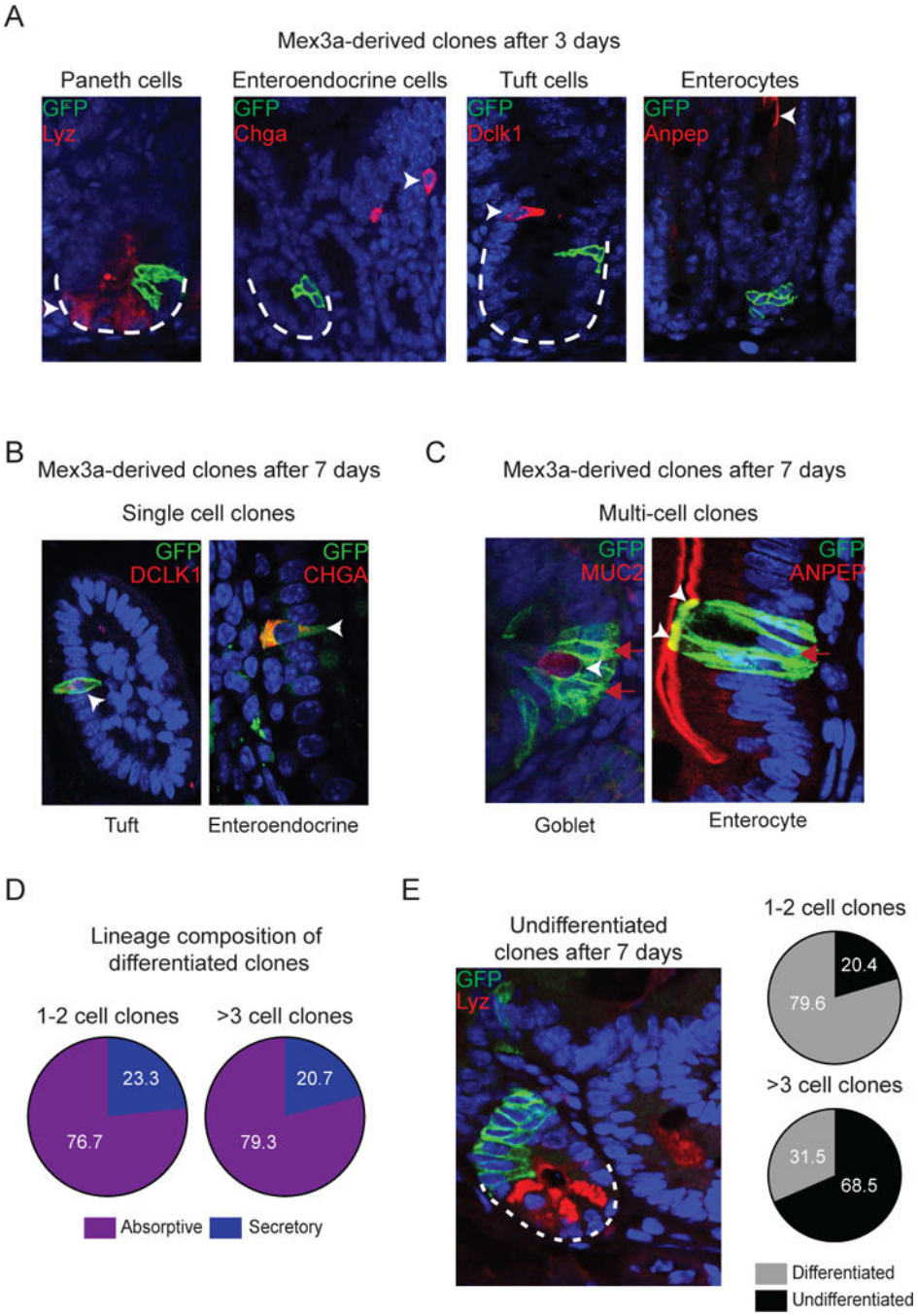

Figure 4. Mex3a cells are a subpopulation of Lgr5+ cells

(A) Representative FACS plot of Lgr5+ cells obtained from compound Mex3a-Tom/+; Lgr5-GFP/+ reporters. Population frequencies are referred to total number of Lgr5::GFP+ cells in the small intestine of compound Lgr5-GFP/+; Mex3a-Tom/+ mice.

(B – D) Characterization of the Lgr5 subpopulations in (A) by RT qPCR analysis of known intestinal cell markers. Relative expression of ISC/Wnt genes (B), high-abundance lineage genes (C), and low-abundance lineage genes (D). Values are normalized to the

subpopulation with the highest expression of each gene. Data represent the mean of 4 independent sorting experiments. (Full expression data is presented in Table S4).
(E) Representative images of 3D cultures containing organoids derived from the Mex3a/Lgr5 subpopulations. Insets show the presence of organoids with high complexity.
(F) Quantification of organoid forming efficiency from Mex3a/Lgr5 subpopulations. Graphs represent the mean ± SEM of organoid efficiency per population obtained from 3 independent sorting experiments (n = 6 cultures per population). *, p val < 0.05; ***, p val < 0.001, in a one-way ANOVA followed by Tukey´s multiple comparison test.
(G) Organoids derived from Mex3a-high Lgr5-high cells were expanded over 30 days to stain for the different intestinal lineages. Organoids showed the presence of stem/progenitor cells (EPHB2), enterocytes (ANPEP+), enteroendocrine cells (CHGA+), Paneth cells (LYZ1+), tuft cells (Dclk1) and goblet cells (MUC2).

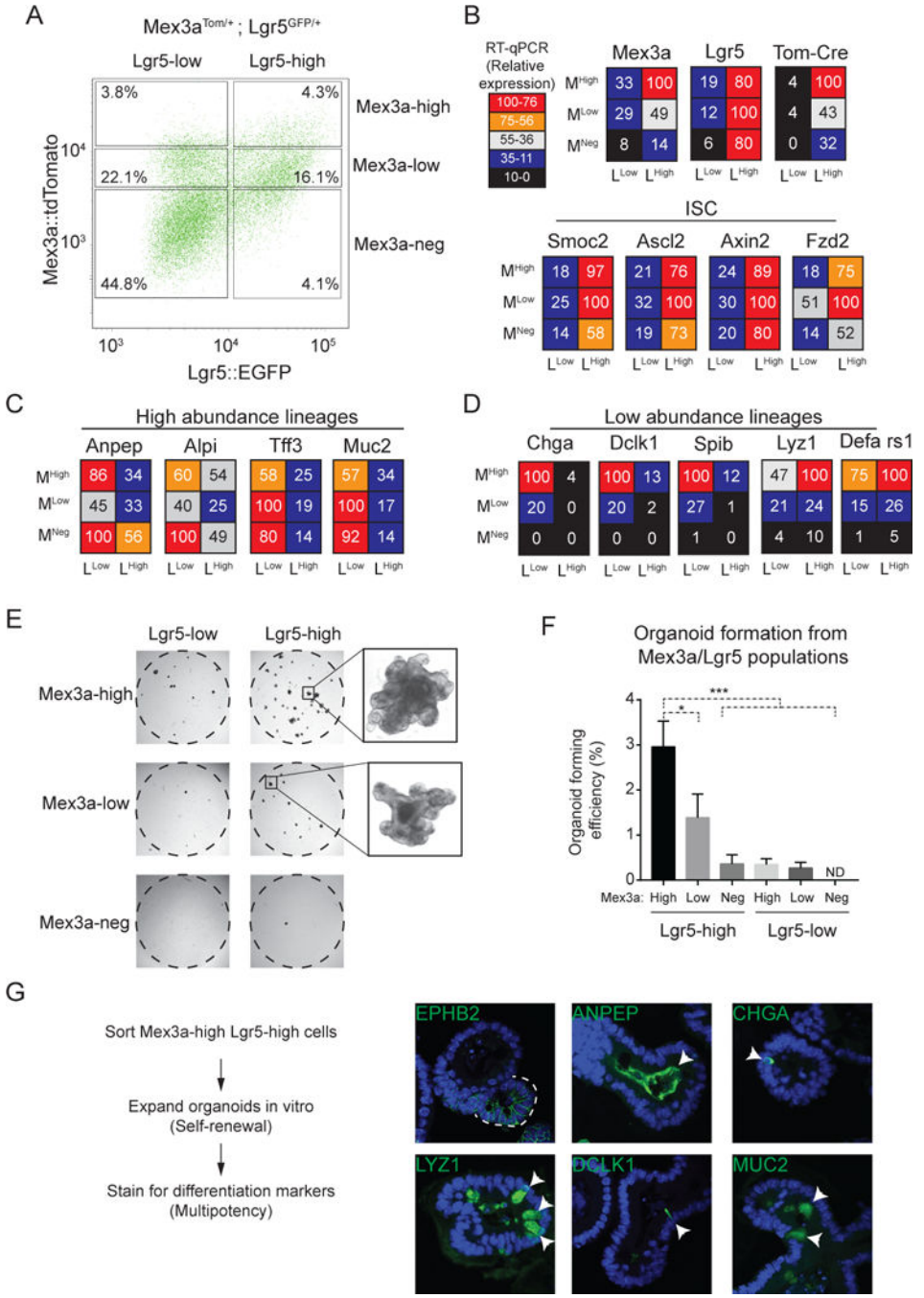

Figure 5. Mex3a-expressing cells are resistant to chemo and radiotherapy

(A) Experimental setup to assess the reponse of Mex3a/Lgr5 subpopulations to stress. Mice were treated twice with either 5-FU (2X 100 mg/kg) or IR (12 Gy) and 48h later small intestines were collected and analyzed by FACS.

(B) Frequency of Lgr5-high cells (left panel) or Mex3a-high cells (right panel) in control and after treatment with 5-FU or IR. Graphs depict the mean ± SD compared to total Lgr5-GFP cells. *, p value < 0.05; ***, p value < 0.001 in a one-way ANOVA followed by Tukey ´s multiple comparison test (n ≥ 4 per group).

(C) Representative FACS plots of GFP+ cells from untreated (left panel), 5-FU treated (middle panel), and IR-treated (right panel) Lgr5-GFP/+; Mex3a-Tom/+ compound mice.
(D) Quantification of Mex3a populations within Lgr5-high cells in control, 5-FU, and IR treated mice. ***, p value < 0.001 in a two-way ANOVA followed by Sidak´s multiple comparison test relative to untreated mice (n ≥ 4 per group).
(E) Quantification of Mex3a populations within Lgr5-low cells in control, 5-FU, and IR treated mice. ***, p value < 0.001 in a two-way ANOVA followed by Sidak´s multiple comparison test relative to untreated mice (n ≥ 4 per group).
(F – G) Mex3a cells increase their cellular output after 5-FU insult. (F) Experimental setup. Tracing was induced with Tamoxifen and followed by two doses of 5-FU. Clones were assessed in control and 5-FU treated mice at 7 and 14 days from the initial tamoxifen treatment. (G) Clone-size distribution at 7 (n = 302 clones for control, n = 170 for 5-FU) and 14 days (n = 331 clones for control, n = 113 clones for 5FU) in control and 5-FU treated mice. All tracing data was obtained from at least 4 mice.

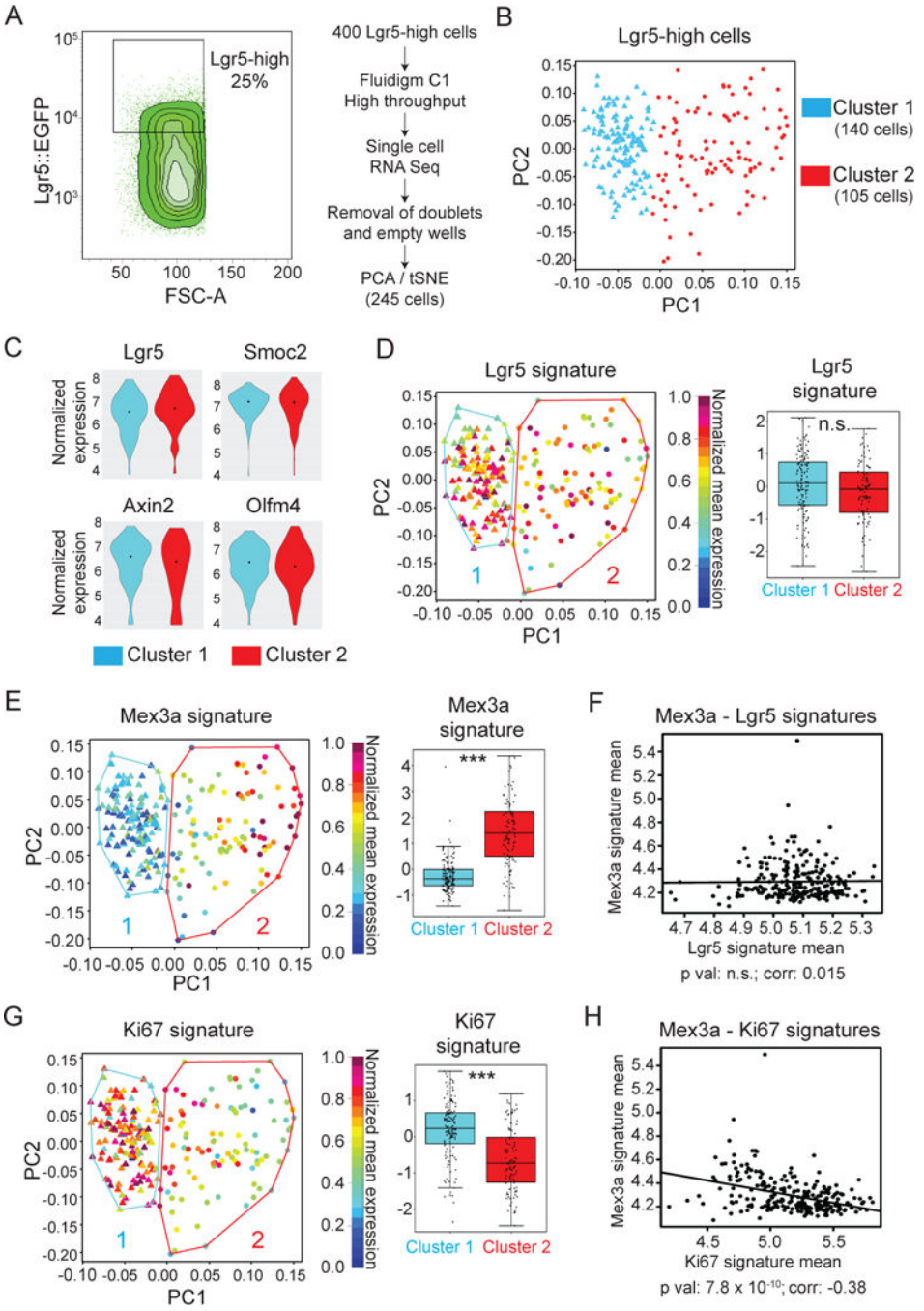

Figure 6. Single cell transcriptomic profiling of Lgr5-high cells identifies a subpopulation enriched in the Mex3a signature

(A) (Left panel) FACS plot used to select for Lgr5-high cells. (Right panel) Experimental setup (See Supplementary Methods for details).

(B) (Left panel) Mean expression of the Lgr5 signature on the tSNE map derived from PCA defined clusters. (Right panel) Box-plot showing the mean ± SD of Lgr5 signature expression in both clusters. n.s, p value > 0.05 in Kruskal-Wallis test.

(C) (Left panel) Mean expression of the Ki67 signature on the tSNE map derived PCA defined clusters. (Right panel) Box-plot showing the mean ± SD of Ki67 signature expression in both clusters. ***, p value < 0.05 in Kruskal-Wallis test.
(D) (Left panel) Mean expression of the Mex3a signature on the tSNE map derived PCA defined clusters. (Right panel) Box-plot showing the mean ± SD of Mex3a signature expression in both clusters. ***, p value < 0.05 in Kruskal-Wallis test.
(E–I) Expression of ISC genes (E), "+4" genes (F), high abundance lineage genes (G), low abundance lineage genes (H), and proliferation genes (I) in Lgr5-high subpopulations. Violin plots show the density and mean expression of each gene.
(J) Correlation between the Mex3a and Lgr5 signatures (left panel), Ki67 and Lgr5 signatures (middle panel), and Mex3a and Ki67 signatures (right panel) in the 245 Lgr5 single cells analyzed by RNA Seq.

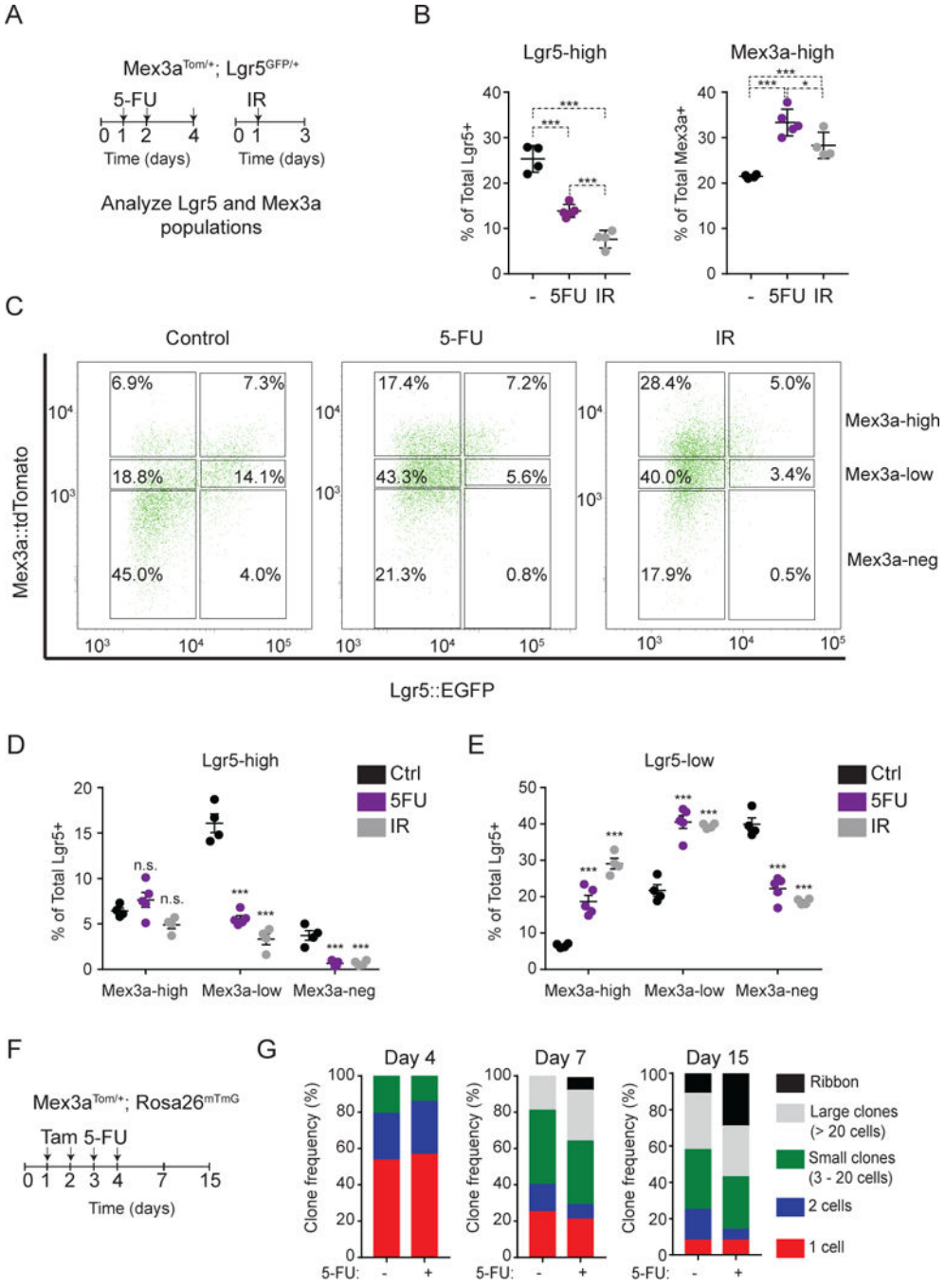

Figure 7.